Conditions for Almost Global Attractivity of a Synchronous Generator Connected to an Infinite Bus

Nikita Barabanov, Johannes Schiffer, Romeo Ortega, Denis Efimov

Conditions for Almost Global Attractivity of a Synchronous Generator Connected to an Infinite Bus

Nikita Barabanov, Johannes Schiffer, Romeo Ortega and Denis Efimov

***Abstract*—Conditions for existence and global attractivity of the equilibria of a realistic model of a synchronous generator with constant field current connected to an infinite bus are derived. First, necessary and sufficient conditions for existence and uniqueness of equilibrium points are provided. Then, sufficient conditions for local asymptotic stability and almost global attractivity of one of these equilibria are given. The analysis is carried out by employing a new Lyapunov–like function to establish convergence of bounded trajectories, while the latter is proven using the powerful theoretical framework of cell structures pioneered by Leonov and Noldus. The efficiency of the derived sufficient conditions is illustrated via extensive numerical experiments based on two benchmark examples taken from the literature.**

***Index Terms*—Power system dynamics, power system stability, nonlinear control systems, cell structures.**

I. Introduction

A. Motivation

Electric energy is the most fundamental energy carrier in modern industrialized societies. To satisfy the electricity demand, power systems have continuously grown to become very large, complex and highly nonlinear systems with an immense variety of actuators, controls and operational constraints [1], [2], [3]. In addition, power systems are persistently being subjected to disturbances, such as changes in load, outages of power plants, or failures in transformer substations and power lines [4]. Consequently, ensuring the stable, reliable and efficient operation of a power system is an enormous, yet crucial, task. This fact becomes even more obvious by noting that already relatively small local disturbances can lead to a cascade of failures, which can cause severe blackouts affecting millions of people [5], [6].

As a result, the problem of power system stability has attracted significant attention by academics and practitioners alike, with the first studies dating back, at least, to the 1920s [7], [8]—see [1, Chapter 1] for a review of the research history on power system stability analysis. However, even today many basic questions remain open. A main reason for this is the complexity of the dynamics of power systems and even their individual components. This forces researchers to invoke several assumptions simplifying the mathematical tasks of stability analysis and control design. Standard assumptions comprise, *e.g.*, neglecting fast dynamics [9], [10], constant voltage amplitudes and small frequency variations [1, Chapter 11]. Such assumptions permit to derive reduced-order synchronous generator (SG) models [1, Chapter 11] and employ algebraic line models [9], [10], simplifying the analysis. Yet most of the employed assumptions are not physically justifiable in generic operation scenarios. In particular, the motion of the machine rotor, *i.e.*, the swing equation, is commonly represented in terms of mechanical and electrical power instead of their corresponding torques. Unfortunately, this approximation is only valid for small frequency variations around the nominal frequency [1], [2], [11]; see also the discussions in [12], [13], [14].

The necessity of improved power systems stability analysis methods has become more compelling in the last few years. Indeed, driven by environmental, economic and societal factors, power systems worldwide are currently undergoing drastic changes and the reliable and efficient integration of large shares of renewable energy sources represents a major technical challenge for the operation of future power systems [15], [16]. One of the main reasons for this is that many renewable energy sources are fluctuating by nature, hence representing an unknown time-varying disturbance to the network. Although there are a variety of concepts and approaches to facilitate the integration of renewable energy sources—*e.g.*, demand-side management, microgrids, smart homes, *etc.* [15], [10]—it is expected that in the future power systems will operate more often closer to their security margins [15], [16]. Therefore, the problem of power system stability can be expected to become even more relevant, making it important to derive easily and quickly verifiable analytic conditions for stability. This is the topic addressed in the present work.

B. Existing literature

As discussed above, one main limitation of current power system stability analysis methods is that they are based on reduced-order models only valid within a limited range of operating conditions. Extending these methods to models containing more accurate representations of the system's components and, hence, being valid in a broader range of operating conditions is a long-standing problem in the power systems literature. Yet only very recently, there has been some progress on providing solutions to this problem. The most relevant contributions are reviewed below.

N. Barabanov is with Department of Mathematics, North Dakota State University, Fargo, ND 58102, USA and Department of Control Systems and Informatics, University ITMO, 49 Avenue Kronverkskiy, 197101 Saint Petersburg, Russia, nikita.barabanov@ndsu.edu

J. Schiffer is with School of Electronic and Electrical Engineering, University of Leeds, Leeds LS2 9JT, UK, j.schiffer@leeds.ac.uk

R. Ortega is with Laboratoire des Signaux et Systémes, École Supérieure d'Electricité (SUPELEC), Gif-sur-Yvette 91192, France and Department of Control Systems and Informatics, University ITMO, 49 Avenue Kronverkskiy, 197101 Saint Petersburg, Russia, ortega@lss.supelec.fr

D. Efimov is with Non-A team@INRIA, Parc Scientifique de la Haute Borne, 40 avenue Halley, 59650 Villeneuve d'Ascq, France, with LAGIS UMR 8219, Ecole Centrale de Lille, Avenue Paul Langevin, 59651 Villeneuve d'Ascq, France and Department of Control Systems and Informatics, University ITMO, 49 avenue Kronverkskiy, 197101 Saint Petersburg, Russia, Denis.Efimov@inria.fr

Version 2, February 6, 2017

In [12] a port-Hamiltonian model of a multi-machine power system with SGs is derived. However, the stability analysis therein is restricted to the special—and unrealistic—case of an SG connected to a constant linear load. In [13] the model proposed in [12] is adopted and a sufficient condition for global asymptotic stability of a generic SG-based power system is derived. However, this stability claim critically relies on the construction of a *unique* steady-state solution of the power system. Unfortunately, this construction is not very realistic, as it is not only based on the assumption of a constant field winding current, but also, and more importantly, on the definition of a very specific value for the mechanical torque of each SG in the system. This torque depends on the constant field current, as well as on an arbitrarily chosen synchronization frequency and arbitrarily pre–specified steady-state terminal voltages for all SGs. The two latter dependencies significantly reduce the practical significance of the considered setup.

A classical, very well known, scenario in the power systems literature is the single–machine infinite bus (SMIB) scenario [11], [2]. Thereby, the infinite bus represents a three-phase voltage source with constant amplitude and frequency and the dynamics contained in the model stem from a single SG [2]. Physically, this scenario is motivated by the assumption that the SG under consideration is connected to a very stiff power system, such that the one generator does not have any influence on the overall network behavior. The SMIB model is often used to illustrate and understand the basic functionality of an SG connected to a power system. It turns out that even for this simplified setup a rigorous analysis is very challenging. Yet, a clear understanding of the SMIB scenario is a fundamental step in the development of a thorough mathematical framework for the analysis of more complex power system dynamics under less restrictive and more realistic assumptions as in [12], [13] or in the classical literature [1], [2], [11]. In addition, the insights that can be gained from the derived conditions can also provide valuable practical conclusions for the design, control and operation of SGs. The same applies to the emerging strand of control concepts that intend to operate grid-connected inverters such that they mimic the dynamics of conventional SGs [17], [18], [19], [20]. This is an interesting approach, because inverter-interfaced units are becoming more and more predominant in the course of growing renewable generation. However, if not properly accounted for, this development may have severe impacts on the network dynamics and stability [15], [16]. In that context, the stability conditions derived in this work could be employed to derive tuning criteria for the control concepts proposed in [17], [18], [19], [20]. The latter objective also has motivated the related works [21], [22], [23].

Motivated by the abovementioned reasons, the present paper is dedicated to the global analysis of the SMIB model containing a detailed nonlinear SG model derived from first principles. By employing the same SG model, the SMIB scenario is also adopted in [21], [22], [23] where sufficient conditions for almost global asymptotic stability (GAS) are derived. The analysis in [21] proceeds along the classical lines of constructing an integro–differential equation resembling the forced pendulum equation and, subsequently, showing that the SMIB system is almost globally asymptotically stable if and only if the same holds for that equation. In [22] the same authors provide slightly simpler conditions for stability resulting from verifying if a real-valued nonlinear map defined on a finite interval is a contraction. But, as stated in [22], these conditions are hard to verify analytically. Furthermore, and perhaps more importantly, the geometric tools employed to establish the results in [21], [22], [23], cannot be extended to a multi–machine power system. In [13] a scenario similar to that of the SMIB system is analyzed. However, as mentioned above, the analysis in [13] is conducted under very stringent assumptions on the specific form of the infinite bus voltage, as well as the admissible values of the mechanical torque.

C. Contributions

In the present paper we focus on the problem of global attractivity of the SMIB model with a detailed SG model derived from first principles. The main contributions of the present paper are as follows.

- Provide a necessary and sufficient condition for uniqueness and existence of equilibria—an essential prerequisite for any convergence or stability analysis. It is shown in the paper that there are, at most, two equilibrium points.
- Derive sufficient conditions for *local* asymptotic stability and *almost global* attractivity of one of these equilibrium points, *i.e.*, for all initial conditions, except a set of measure zero, the solutions of the SMIB system tend to that equilibrium point.
- Evaluate the effectiveness of the conditions via extensive numerical experiments based on two benchmark examples.

Our results differ from the ones in [21], [22], [13], [23] in the following aspects. First, to construct the error system we employ a coordinate transformation that only depends on the system's stationary electrical frequency, but is independent of the specific phase angle of any electrical network quantity. This is common practice in modeling of reduced-order phasor-based multi-machine power systems [2], [10] and has the advantage that the employed approaches are scalable in the sense that they are applicable—with a suitably modified, but structurally similar, Lyapunov-like function—to large multi-machine systems. Second, we don't rely on any of the questionable assumptions made in [13].

At this point, it seems convenient to clarify two important technical issues regarding the conventions employed in the present paper compared to those in [21], [22], [13], [23]. First, the equilibrium of the SMIB model considered in the paper *cannot* be rendered GAS via continuous feedback, hence the need for the qualifier "almost"[1]. As a matter of fact, the SMIB system is naturally defined on the torus, which is not diffeomorphic to the Euclidean space, and GAS is hampered by a well known topological obstruction [24]. Second, the analysis carried out in the paper *does not* rely on the construction of a *bona fide* Lyapunov function. Consequently, it is not proven that the equilibrium is GAS, but only almost globally

[1]Almost GAS means that for all initial conditions, except a set of Lebesgue measure zero, the trajectories will converge to the equilibrium.

attractive. Furthermore, in order to establish this result, it is necessary to unfold the torus and work with the angles defined in Euclidean space. In turn, this implies that the angles are not bounded by definition and, hence, boundedness of solutions of the SMIB system has to be proven.

The present work extends our previous results in [25] in several regards. Namely, we provide physical interpretations of part of our conditions; the proofs of the main theoretical contributions are presented in more detail; we provide extensive numerical experiments illustrating the usefulness of our approach.

The remainder of the paper is structured as follows. In Section II, the SMIB model is introduced. The steady-state solutions of this model are investigated in Section III. Therein, it is shown that there are, at most, two equilibrium points (modulo 2π). To establish the global attractivity result, we first construct in Section IV a new Lyapunov–like function—*i.e.*, a function that *is not positive definite* but whose derivative is negative semi–definite and establish convergence of bounded trajectories by invoking LaSalle's invariance principle [26]. To ensure boundedness of solutions, we recall the powerful, yet little known, theoretical framework of cell structures pioneered by Leonov and co–workers [27], [28], [29], [30] as well as Noldus [31] in Section V. Finally, in Section VI we combine the results of Sections IV and V to give conditions on the SMIB system parameters under which the cell structure principle is satisfied, hence completing the almost global attractivity analysis. Section VII presents two benchmark simulation examples illustrating the theoretical results. The paper is summarized in Section VIII where an outlook on future work is also given.

II. Model of a synchronous generator connected to an infinite bus

The main equations and assumptions for the considered SMIB system are given in this section. The employed assumptions on the SG are standard [32], [17] and also used in [13], [21], [22], [23]. First, the rotor is round, the machine has one pole pair per phase, there are no damper windings and no saturation effects as well as no Eddy currents. Second, we assume that the rotor current i_f is a real constant. Third, we assume balanced or, equivalently, symmetric three-phase signals throughout the paper [10, Definition 2.3]. For the SG this is equivalent to assuming a "perfectly built" machine connected in star with no neutral line, as in [21], [22].

Following the notation and modeling in [32], we employ a generator reference direction, *i.e*, current flowing out of the SG terminals is counted positively. The electrical rotor angle of the SG is denoted by[2] $\delta : \mathbb{R}_{\geq 0} \to \mathbb{R}$ and the electrical frequency by $\omega = \dot{\delta}$. Here, δ is the angle between the axis of coil a of the SG and the d-axis, see Fig. 1. With a constant rotor current i_f, the three-phase electromotive force (EMF) $e_{abc} : \mathbb{R}_{\geq 0} \to \mathbb{R}^3$ is given by [32], [17]

$$e_{abc} = M_f i_f \omega \begin{bmatrix} \sin(\delta) \\ \sin(\delta - \frac{2\pi}{3}) \\ \sin(\delta + \frac{2\pi}{3}) \end{bmatrix}, \tag{1}$$

where $M_f \in \mathbb{R}_{>0}$ is the peak mutual inductance. The three-phase voltage at the infinite bus is denoted by

$$v_{abc} := \sqrt{2} V \begin{bmatrix} \sin(\delta_g) \\ \sin(\delta_g - \frac{2\pi}{3}) \\ \sin(\delta_g + \frac{2\pi}{3}) \end{bmatrix}, \tag{2}$$

where $V \in \mathbb{R}_{>0}$ is the root-mean-square (RMS) value of the constant voltage amplitude (line-to-neutral) and

$$\delta_g = \delta_g(0) + \omega^s t \in \mathbb{R} \tag{3}$$

with the grid frequency ω^s being a positive real constant. The stator resistance and inductance are denoted by $R \in \mathbb{R}_{>0}$, respectively $L = L_s + M_s$, where $L_s \in \mathbb{R}_{>0}$ is the self-inductance and $M_s \in \mathbb{R}_{>0}$ the mutual inductance. Moreover, in the SMIB model the inductance and resistance of the transmission line connecting the SG to the infinite bus are included in the parameters L and R, see [2, Section 4.13.1]. With these considerations, the *electrical* equations describing the dynamics of the three-phase stator current $i_{abc} : \mathbb{R}_{\geq 0} \to \mathbb{R}^3$ are given by

$$L \frac{di_{abc}}{dt} = -R i_{abc} + e_{abc} - v_{abc}. \tag{4}$$

The *mechanical* equations describing the rotor dynamics, *i.e.*,

$$\begin{aligned} \dot{\delta} &= \omega, \\ J\dot{\omega} &= -D\omega + T_m - T_e, \end{aligned} \tag{5}$$

complete the SMIB model. Here, $J \in \mathbb{R}_{>0}$ is the total moment of inertia of the rotor masses, $D \in \mathbb{R}_{>0}$ is the damping coefficient[3] and $T_m \in \mathbb{R}_{\geq 0}$ is the mechanical torque provided by the prime mover. Furthermore, we assume T_m constant throughout the paper. Finally, the electrical torque T_e can be expressed as [17]

$$T_e = \omega^{-1} i_{abc}^\top e_{abc}. \tag{6}$$

For our analysis, we choose to represent all three-phase electrical variables in dq-coordinates. To this end, we employ the dq-transformation given in Appendix A with the transformation angle

$$\varphi := \omega^s t. \tag{7}$$

The angle difference between the rotor angle δ and the dq-transformation angle φ is denoted by

$$\theta := \delta - \varphi.$$

Hence, the grid voltage (2) is given by the following *constant* vector in dq-coordinates (see [10]),

$$v_{dq} = \begin{bmatrix} v_d \\ v_q \end{bmatrix} = \sqrt{3} V \begin{bmatrix} \sin(\delta_g - \varphi) \\ \cos(\delta_g - \varphi) \end{bmatrix} = \sqrt{3} V \begin{bmatrix} \sin(\delta_g(0)) \\ \cos(\delta_g(0)) \end{bmatrix},$$

where the second equality follows from (3). Furthermore, with

$$b := \sqrt{3/2} M_f i_f, \tag{8}$$

[2] See Remark 1.

[3] Please see Section VII for a discussion of the physical meaning of the coefficient D.

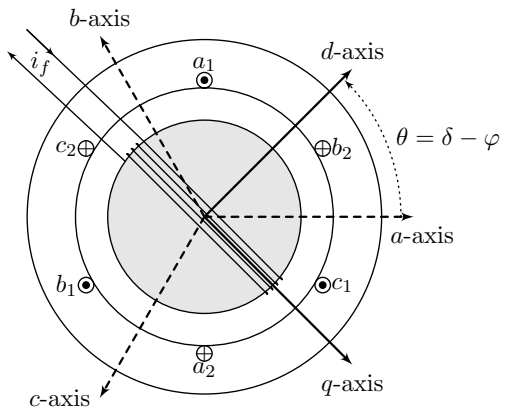

Fig. 1: Schematic representation of a two-pole round-rotor SG based on [32, Figure 3.2]. The abc-axes correspond to the axes of the stator coils denoted by $a_{1,2}$, $b_{1,2}$ and $c_{1,2}$. The axis of coil a is chosen at $\theta = \delta - \varphi = 0$. The rotor current i_f flows through the rotor windings. The dq-axes denote the rotating axes of the dq-frame corresponding to the mapping $T_{dq}(\varphi)$ with φ given in (7) and $T_{dq}(\cdot)$ given in Appendix A.

the EMF in dq-coordinates is given by

$$e_{dq} = \begin{bmatrix} e_d \\ e_q \end{bmatrix} = \begin{bmatrix} b\omega \sin(\theta) \\ b\omega \cos(\theta) \end{bmatrix}. \tag{9}$$

Note that the electrical torque T_e in (6) is given in dq-coordinates by

$$T_e = \omega^{-1} i_{dq}^\top e_{dq} = b(i_q \cos(\theta) + i_d \sin(\theta)) \tag{10}$$

and that, with φ given in (7) and $T_{dq}(\cdot)$ given in Appendix A,

$$\frac{dT_{dq}(\varphi)}{dt} i_{abc} = \omega^s \begin{bmatrix} -i_q \\ i_d \end{bmatrix},$$

see [10, equation (4.8)]. Hence, by replacing the rotor angle dynamics, *i.e.*, $\dot{\delta}$, with the relative rotor angle dynamics, *i.e.*, $\dot{\theta}$, the SMIB model given by (4), (5) and (6) becomes in dq-coordinates

$$\begin{aligned} \dot{\theta} &= \omega - \omega^s, \\ J\dot{\omega} &= -D\omega + T_m - b\left(i_q \cos(\theta) + i_d \sin(\theta)\right), \\ L\dot{i}_d &= -Ri_d - L\omega^s i_q + b\omega \sin(\theta) - v_d, \\ L\dot{i}_q &= -Ri_q + L\omega^s i_d + b\omega \cos(\theta) - v_q. \end{aligned} \tag{11}$$

The model (11) is used for the analysis in this paper.

Remark 1. *To establish an important result of this paper, namely that all bounded solutions converge to an equilibrium, it is necessary to—unfolding the torus where the system lives naturally—work with the angles defined on the real line rather than on the circle. This technical step is required in order to construct a continuous Lyapunov-like function for the system* (11)*. However, the Lyapunov-like analysis does not allow us to conclude that the coordinate θ in* (11) *is bounded. Therefore, the latter property is established by using the framework of cell structures [31], [27], [28], [29] in Section V.*

Remark 2. *In [13], [21], [22], the dq-transformation angle φ is chosen as the rotor angle,* i.e.*, $\varphi = \delta$. This yields $e_d = 0$ in* (9)*. In addition, in [21], [22] a dq-transformation is chosen in which the d-axis lags the q-axis by $\pi/2$. In our notation, this coordinate frame can be obtained by setting the transformation angle to $\varphi = \delta + \pi$. Hence, $e_q = b\omega$ in [13] and $e_q = -b\omega$ in [21], [22].*

Remark 3. *The analysis reported in the paper can be conducted in any coordinate frame. However, we favor the one used here since it seems to be more suitable to extend the results to the multi-machine case.*

III. Existence and uniqueness of equilibria

This section is dedicated to deriving conditions on existence and uniqueness of equilibria of the system (11), which we denote by $(\theta^s, \omega^s, i_d^s, i_q^s)$. To simplify the notation it is convenient to introduce two important constants

$$\begin{aligned} c &:= b\sqrt{(v_d^2 + v_q^2)((L\omega^s)^2 + R^2)}, \\ \mathcal{P} &:= \frac{1}{c}\left[-b^2\omega^s R + (T_m - D\omega^s)((L\omega^s)^2 + R^2)\right]. \end{aligned} \tag{12}$$

It is clear from (8) that c is nonzero if the rotor current i_f is nonzero, which is satisfied in any practical scenario.

Proposition 1. *The system in* (11) *possesses two unique steady-state solutions (modulo 2π) if and only if*

$$|\mathcal{P}| < 1. \tag{13}$$

If and only if (13) *is satisfied with equality, the system* (11) *has exactly one steady-state solution (modulo 2π).*

Proof. Obviously, the equilibria of the system (11) are 2π-periodic in θ. Furthermore, we have to solve the equations

$$\begin{aligned} \omega - \omega^s &= 0, \\ -D\omega - bi_d \sin(\theta) - bi_q \cos(\theta) + T_m &= 0, \\ -Ri_d - L\omega^s i_q + b\omega \sin(\theta) - v_d &= 0, \\ L\omega^s i_d - Ri_q + b\omega \cos(\theta) - v_q &= 0. \end{aligned} \tag{14}$$

It is straightforward to check that equilibria $(\theta^s, \omega^s, i_d^s, i_q^s)$ are given by

$$\begin{aligned} \omega^s &= \omega^s, \\ i_d^s &= \frac{bR\omega^s \sin(\theta^s) - bL(\omega^s)^2 \cos(\theta^s) - v_d R + v_q L\omega^s}{(L\omega^s)^2 + R^2}, \\ i_q^s &= \frac{(\omega^s)^2 Lb \sin(\theta^s) + \omega^s bR \cos(\theta^s) - v_d L\omega^s - v_q R}{(L\omega^s)^2 + R^2}, \\ &b(L\omega^s v_q - Rv_d)\sin(\theta^s) - b(L\omega^s v_d + Rv_q)\cos(\theta^s) \\ &= -b^2\omega^s R + (T_m - D\omega^s)((L\omega^s)^2 + R^2). \end{aligned} \tag{15}$$

Some trigonometric manipulations of the left-hand side of the last equation yield

$$\begin{aligned} &b(L\omega^s v_q - Rv_d)\sin(\theta^s) - b(L\omega^s v_d + Rv_q)\cos(\theta^s) = \\ &= b\sqrt{(v_d^2 + v_q^2)((L\omega^s)^2 + R^2)}\sin(\theta^s - \phi), \end{aligned}$$

where

$$\phi = \arctan\left(\frac{L\omega^s v_d + Rv_q}{L\omega^s v_q - Rv_d}\right), \tag{16}$$

and $\arctan(\cdot)$ denotes the standard arctangent function with range in the interval $[0, \pi)$. Note that, by definition of v_d and v_q, the case $v_d = v_q = 0$ is excluded and, hence, ϕ is well-defined.

With these considerations, and by rearranging terms, the last equation in (15) implies that solutions θ^s exist if and only if

$$\left| \frac{-b^2\omega^s R + (T_m - D\omega^s)((L\omega^s)^2 + R^2)}{b\sqrt{(v_d^2 + v_q^2)((L\omega^s)^2 + R^2)}} \right| \leq 1, \tag{17}$$

which is precisely condition (13). Thus, condition (17) is necessary and sufficient for system (11) to have either one (equality) or exactly two (strict inequality) equilibria (modulo 2π), completing the proof. □

A related analysis of existence and uniqueness of equilibria of the model (11) is reported in [13, Section III.E]. Yet, therein the admissible mechanical torque T_m is restricted to a specific function $T_m = T_m(b, D, \omega^s, L, R, v_d, v_q)$. This parametric restriction is needed to ensure existence of exactly one single equilibrium point of the system (11) and is essential for the subsequent GAS analysis in [13]. Compared to this, the present analysis merely requires (13) to be satisfied, hence being significantly less restrictive and practically more realistic. Also, we emphasize that the topological properties of the model (11) prevent any of its equilibria being GAS [24]. The GAS claim in [13] can only be established, because the dynamics of the angle θ in (11) are omitted from the analysis.

In [21], [22], no explicit analysis of existence and uniqueness of equilibria is performed, but it is claimed that for a sufficiently large infinite bus amplitude V there always are two equilibria. This claim can be made rigorous by inspection of (17), which clearly can be satisfied for sufficiently large $V = 1/3\sqrt{v_d^2 + v_q^2}$.

To provide a physical interpretation of condition (13), it is convenient to introduce some constants following standard definitions in power systems. More precisely, we define the reactance X, the conductance G, the susceptance B and the admittance Y as

$$\begin{aligned} &X := \omega^s L,\ G := \frac{R}{R^2 + X^2},\ B := -\frac{X}{R^2 + X^2}, \\ &Y := G + jB,\ |Y| = \sqrt{G^2 + B^2}, \end{aligned} \tag{18}$$

Moreover, we define the admittance angle as

$$\beta := \arctan\left(\frac{G}{B}\right), \tag{19}$$

and denote the amplitude of the EMF e_{abc} in (1) by

$$E := \frac{1}{\sqrt{2}}\omega m i_f = \frac{1}{\sqrt{3}}\omega b. \tag{20}$$

We have the following relation between the electrical torque T_e in (10) and the active power P, *i.e.*, the amount of power transformed from mechanical power to electrical power with some of it being lost in the resistance of the stator coils [1],

$$P = \omega T_e.$$

Multiplying condition (13) on both sides with $|\omega^s c|$ yields

$$|\mathcal{P} c\omega^s| < |c\omega^s|. \tag{21}$$

By using the relations introduced above, we obtain

$$\begin{aligned} \mathcal{P} c\omega^s &= -(b\omega^s)^2 R + (T_m - D\omega^s)\omega^s(X^2 + R^2) \\ &= |Y|^{-2}\left(-3E^2 G + P_m - P_D\right), \end{aligned} \tag{22}$$

where we introduced the *steady-state* mechanical power $P_m = T_m\omega^s$ and the *steady-state* damping power $P_D = D(\omega^s)^2$. Also,

$$\begin{aligned} c\omega^s &= \omega^s b V\sqrt{3}|Y|^{-1} \\ &= 3EV|Y|^{-1}. \end{aligned} \tag{23}$$

Hence, with (22) and (23), (21) becomes

$$|-3E^2 G + P_m - P_D| < 3|(EV|Y|)|. \tag{24}$$

We recall that the stationary power flow P_L over the power line connecting the SG and the infinite bus is given by

$$P_L = 3EV|Y|\sin(\theta^s - \delta_g(0) + \beta), \tag{25}$$

where β is defined in (19). Consequently, we see from (24) that condition (17) has the physical interpretation that the mechanical power provided by the machine must not exceed the power dissipated through damping (P_D), internal losses ($3E^2G$) and transmission (P_L), *i.e.*, for an equilibrium to exist a stationary power balance must be possible. A similar observation has been made for first-order droop-controlled inverters in [33].

IV. Convergence of *Bounded* Solutions

In this section, a sufficient condition under which all *bounded* solutions of the system (28) converge to an equilibrium is derived. The claim is established by constructing a Lyapunov–like function and invoking LaSalle's invariance principle [26].

Throughout the rest of the paper we make the following natural assumption.

Assumption 1. *The parameters of the system* (11) *are such that condition* (13) *of Proposition 1 is satisfied and* $i_f > 0$.

As seen from (8), the signs of c and, hence, $\mathcal{P}$ defined in (12) depend on the sign of the constant rotor current i_f. For the subsequent analysis, it is important to know the sign of c, as it determines which of the two equilibria of the system (11) is stable. Assumption 1 is made without loss of generality because, as seen below, the analysis for $i_f < 0$ follows *verbatim*—see the numerical example in Section VII.

Proposition 2. *Consider the system* (11) *verifying Assumption 1 and the inequality*

$$4RD[(L\omega^s)^2 + R^2] > (Lb\omega^s)^2. \tag{26}$$

Every bounded solution tends to an equilibrium point.

Proof. Assumption 1 ensures the existence of equilibria. As usual, it is convenient to first shift one of the (infinitely

many) equilibrium points to the origin via the the change of coordinates

$$\theta = \tilde{\theta} + \theta^s, \;\; \omega = \tilde{\omega} + \omega^s, \;\; i_d = \tilde{i}_d + i_d^s, \;\; i_q = \tilde{i}_q + i_q^s.$$

In the incremental variables $(\tilde{\theta}, \tilde{\omega}, \tilde{i}_d, \tilde{i}_q)$ the system (11) has the form

$$\begin{aligned}
\dot{\tilde{\theta}} =& \tilde{\omega}, \\
J\dot{\tilde{\omega}} =& - D(\tilde{\omega} + \omega^s) - b(i_d^s + \tilde{i}_d)\sin(\theta^s + \tilde{\theta}) \\
& - b(i_q^s + \tilde{i}_q)\cos(\theta^s + \tilde{\theta}) + T_m, \\
L\dot{\tilde{i}}_d =& - R(i_d^s + \tilde{i}_d) - L\omega^s(i_q^s + \tilde{i}_q) \\
& + b(\tilde{\omega} + \omega^s)\sin(\theta^s + \tilde{\theta}) - v_d, \\
L\dot{\tilde{i}}_q =& - R(i_q^s + \tilde{i}_q) + L\omega^s(i_d^s + \tilde{i}_d) \\
& + b(\tilde{\omega} + \omega^s)\cos(\theta^s + \tilde{\theta}) - v_q.
\end{aligned} \tag{27}$$

Furthermore, taking into account equations (15), we get

$$\begin{aligned}
\dot{\tilde{\theta}} =& \tilde{\omega}, \\
J\dot{\tilde{\omega}} =& - D\tilde{\omega} - b\tilde{i}_d\sin(\theta^s + \tilde{\theta}) - bi_d^s(\sin(\theta^s + \tilde{\theta}) - \sin(\theta^s)) \\
& - b\tilde{i}_q\cos(\theta^s + \tilde{\theta}) - bi_q^s(\cos(\theta^s + \tilde{\theta}) - \cos(\theta^s)), \\
L\dot{\tilde{i}}_d =& - R\tilde{i}_d - L\omega^s\tilde{i}_q + b\omega^s(\sin(\theta^s + \tilde{\theta}) - \sin(\theta^s)) \\
& + b\tilde{\omega}\sin(\theta^s + \tilde{\theta}), \\
L\dot{\tilde{i}}_q =& - R\tilde{i}_q + L\omega^s\tilde{i}_d + b\omega^s(\cos(\theta^s + \tilde{\theta}) - \cos(\theta^s)) \\
& + b\tilde{\omega}\cos(\theta^s + \tilde{\theta}).
\end{aligned} \tag{28}$$

The second step is to construct the Lyapunov–like function. To this end, note that the electrical dynamics takes the form

$$L\dot{\tilde{i}}_{dq} = \begin{bmatrix} u \\ w \end{bmatrix} + \begin{bmatrix} b\tilde{\omega}\sin(\theta^s + \tilde{\theta}) \\ b\tilde{\omega}\cos(\theta^s + \tilde{\theta}) \end{bmatrix}, \tag{29}$$

where we defined

$$\begin{bmatrix} u \\ w \end{bmatrix} := \begin{bmatrix} -R & -L\omega^s \\ L\omega^s & -R \end{bmatrix} \tilde{i}_{dq} + \begin{bmatrix} b\omega^s(\sin(\tilde{\theta} + \theta^s) - \sin(\theta^s)) \\ b\omega^s(\cos(\tilde{\theta} + \theta^s) - \cos(\theta^s)) \end{bmatrix}.$$

From the expression above we see that including a term in $\frac{L}{2}(u^2 + w^2)$ in the Lyapunov-like function candidate generates a "good" term $-R|\tilde{i}_{dq}|^2$ in its derivative. This together with a detailed inspection of (28) suggests the following function

$$\begin{aligned}
V(\chi) =& \frac{L}{2}(u^2 + w^2) + \frac{J\tilde{\omega}^2}{2}\left[(L\omega^s)^2 + R^2\right] \\
& + b^2 R\omega^s(\tilde{\theta} - \sin\tilde{\theta}) + L(b\omega^s)^2(1 - \cos\tilde{\theta}) \\
& + b\left[(L\omega^s)^2 + R^2\right]\left[i_d^s\left(\cos\theta^s - \cos(\tilde{\theta} + \theta^s) - \tilde{\theta}\sin\theta^s\right)\right. \\
& \left. + i_q^s\left(\sin(\tilde{\theta} + \theta^s) - \sin\theta^s - \tilde{\theta}\cos\theta^s\right)\right],
\end{aligned} \tag{30}$$

where we defined the four–dimensional state vector

$$\chi := (\tilde{\theta}, \tilde{\omega}, \tilde{i}_d, \tilde{i}_q).$$

Some lengthy, but straightforward, calculations show that

$$\begin{aligned}
\dot{V} =& - R[u^2 + w^2] - D((L\omega^s)^2 + R^2)\tilde{\omega}^2 + \\
& + \tilde{\omega}u\, Lb\omega^s\cos(\tilde{\theta} + \theta^s) - \tilde{\omega}w\, Lb\omega^s\sin(\tilde{\theta} + \theta^s) \\
=& \begin{bmatrix} u & w & \tilde{\omega} \end{bmatrix} M \begin{bmatrix} u & w & \tilde{\omega} \end{bmatrix}^\top,
\end{aligned} \tag{31}$$

where we defined the matrix

$$M := \begin{bmatrix} -R & 0 & \frac{Lb\omega^s\cos(\tilde{\theta}+\theta^s)}{2} \\ 0 & -R & -\frac{Lb\omega^s\sin(\tilde{\theta}+\theta^s)}{2} \\ \frac{Lb\omega^s\cos(\tilde{\theta}+\theta^s)}{2} & -\frac{Lb\omega^s\sin(\tilde{\theta}+\theta^s)}{2} & -D((L\omega^s)^2 + R^2) \end{bmatrix}. \tag{32}$$

A simple Schur complement analysis shows that $M < 0$ if and only if (26) holds.

Now, by LaSalle's invariance principle [26] all bounded solutions of the system (28) converge to the largest invariant set contained in the set $\{\chi \in \mathbb{R}^4 : \dot{V} = 0\}$. Clearly,

$$\dot{V} = 0 \;\Leftrightarrow\; w = u = \tilde{\omega} = 0.$$

Hence, $\tilde{\theta}$ is constant and, from (29), we have that $\tilde{i}_{dq}$ is also constant. Consequently, the set $\{\chi \in \mathbb{R}^4 : \dot{V} = 0\}$ is an equilibrium set, completing the proof. □

Remark 4. *The function V given in* (30) *contains a linear term in $\tilde{\theta}$, which makes V discontinuous if we define the system on the torus. See Remark 1.*

Remark 5. *With* (18)*, condition* (26) *can be rewritten as*

$$4DG(R^2 + X^2)^2 > X^2b^2 \quad \Leftrightarrow \quad 4D\frac{R}{X} > |B|b^2.$$

This shows that a high damping factor D and a high R/X ratio, i.e.*, a high electrical dissipation, are beneficial to ensure convergence. On the contrary, a high value of $|b|$,* i.e.*, a high excitation and consequently large EMF amplitude, deteriorate the likelihood of convergence. Both observations are sensible from a physical perspective and consistent with practical experience.*

V. Boundedness of Solutions

In this section, we establish a key requirement to invoke the convergence result of Proposition 2, namely boundedness of solutions. As indicated in Remark 4 to ensure continuity of the function V, we are viewing the system evolving in $\mathbb{R}^4$. Therefore $\tilde{\theta}$ is not a–priori bounded. To prove this fact we use the cell structure principle of Leonov and co–workers [27], [28], [29], [30] as well as Noldus [31]. Although the proof of the proposition is an immediate corollary of Theorem 16 in [30, Chapter 8], (see also [29]), it is given here for the sake of completeness.

Proposition 3. *Consider the function V defined in* (30)*. Assume there exist positive numbers ϵ and λ such that along the solutions of the system* (28) *the function*

$$\bar{V} := V - \frac{\epsilon}{2}\tilde{\theta}^2 \tag{33}$$

verifies

$$\dot{\bar{V}} \leq -\lambda\bar{V}. \tag{34}$$

Then, all solutions $(\tilde{\theta}, \tilde{\omega}, \tilde{i}_d, \tilde{i}_q)$ of the system (28) are bounded.

Proof. Note that from (30) and (31) we have that the evolution of u, w and $\tilde{\omega}$—along solutions of the system (28)—is bounded. This implies that $\tilde{i}_{dq}$ is also bounded and it only remains to show that $\tilde{\theta}$ is bounded. To show the latter, we begin by simplifying the function V defined in (30). Recall from (16) that by definition, ϕ is the unique number in $[0, \pi)$ such that

$$\begin{aligned} \cos\phi =& \frac{b}{c}(L\omega^s v_q - R v_d), \\ \sin\phi =& \frac{b}{c}(L\omega^s v_d + R v_q), \end{aligned} \tag{35}$$

where the constant c is defined in (12). Together with (15), we have that

$$\begin{aligned} & b^2 R\omega^s(\tilde{\theta} - \sin\tilde{\theta}) + L(b\omega^s)^2(1-\cos\tilde{\theta}) + \\ & + b\left[(L\omega^s)^2 + R^2\right]\left[i_d^s\left(\cos\theta^s - \cos(\tilde{\theta}+\theta^s) - \tilde{\theta}\sin\theta^s\right) + \right. \\ & \left. + i_q^s\left(\sin(\tilde{\theta}+\theta^s) - \sin\theta^s - \tilde{\theta}\cos\theta^s\right)\right] = \\ & c\int_0^{\tilde{\theta}} [\sin(\theta^s - \phi + s) - \sin(\theta^s - \phi)]ds. \end{aligned}$$

Hence, V can be written compactly as

$$\begin{aligned} V(\chi) =& \frac{L}{2}(u^2+w^2) + \frac{J\tilde{\omega}^2}{2}((L\omega^s)^2 + R^2) + \\ & + c\int_0^{\tilde{\theta}} [\sin(\theta^s - \phi + s) - \sin(\theta^s - \phi)]ds. \end{aligned} \tag{36}$$

From the definition of V in (36) it follows that the function $\bar{V}$ is positive definite on the hyperplane $\tilde{\theta} = 0$. For every integer $k = 0, \pm 1, \pm 2, \ldots$ consider the function

$$\begin{aligned} \bar{V}_k(\chi) =& \frac{L}{2}(u^2+w^2) + \frac{J\tilde{\omega}^2}{2}((L\omega^s)^2 + R^2) - \frac{\epsilon}{2}(\tilde{\theta} - 2\pi k)^2 \\ & + c\int_{2\pi k}^{\tilde{\theta}} [\sin(\theta^s - \phi + s) - \sin(\theta^s - \phi)]ds. \end{aligned} \tag{37}$$

It follows immediately that $\bar{V}_k$ is positive definite on the hyperplane $\tilde{\theta} = 2\pi k$. In addition, by denoting

$$\tilde{\chi} = \chi - 2\pi k[1\ 0\ 0\ 0]^\top,$$

we have from (37) that for any integer k,

$$\bar{V}(\tilde{\chi}) = \bar{V}_k(\chi).$$

Furthermore, by writing (28) as

$$\dot{\chi} = f(\chi),$$

we see that the periodicity of the dynamics (28) in $\tilde{\theta}$ implies that

$$\dot{\chi} = f(\chi) = f(\tilde{\chi}).$$

Hence, evaluating the time derivative of $\bar{V}_k$ along solutions of the system (28) yields

$$\begin{aligned} \dot{\bar{V}}_k &= \frac{\partial \bar{V}_k(\chi)}{\partial \chi} f(\chi) = \frac{\partial \bar{V}_k(\chi)}{\partial \chi} f(\chi - 2\pi k[1\ 0\ 0\ 0]^\top) \\ &= \frac{\partial \bar{V}(\chi - 2\pi k[1\ 0\ 0\ 0]^\top)}{\partial \chi} f(\tilde{\chi}). \end{aligned}$$

Since $\partial\tilde{\chi} = \partial\chi$ and $\dot{\bar{V}} \leq -\lambda\bar{V}$ by assumption, we obtain

$$\begin{aligned} \dot{\bar{V}}_k &= \frac{\partial \bar{V}(\tilde{\chi})}{\partial \tilde{\chi}} f(\tilde{\chi}) \\ &\leq -\lambda \bar{V}(\tilde{\chi}) \\ &= -\lambda \bar{V}_k(\chi). \end{aligned}$$

Hence, the fact that by assumption $\dot{\bar{V}} \leq -\lambda\bar{V}$, *i.e.*, condition (34), implies that also for every integer k,

$$\dot{\bar{V}}_k \leq -\lambda \bar{V}_k.$$

This together with the 2π-periodicity of the system (28) with respect to $\tilde{\theta}$, implies that for every integer k the set

$$Z_k = \{\chi \in \mathbb{R}^4 : \bar{V}_k(\chi) \leq 0\} \tag{38}$$

is invariant with respect to solutions of the system (28).

Assume $\chi(\cdot)$ is a solution of system (28) with initial condition $\chi(0) = \chi_0$. From the definition of the function $\bar{V}_k$ in (37) we see that $\bar{V}_k(\chi_0)$ is decreasing with respect to $|k|$ quadratically. Hence, for any χ_0 there exist integers k_1 and k_2, with $k_1 < k_2$, such that $\bar{V}_{k_1}(\chi_0) \leq 0$, $\tilde{\theta}(0) \geq 2\pi k_1$, and $\bar{V}_{k_2}(\chi_0) \leq 0$, $\tilde{\theta}(0) \leq 2\pi k_2$. The function $\bar{V}_{k_1}$ is positive on the plane $\tilde{\theta} = 2\pi k_1$, and the function $\bar{V}_{k_2}$ is positive on the plane $\tilde{\theta} = 2\pi k_2$. Furthermore, the sets Z_{k_1} and Z_{k_2} are invariant. Consequently, we have that

$$2\pi k_1 \leq \tilde{\theta}(t) \leq 2\pi k_2$$

for all $t \geq 0$. This completes the proof. □

Remark 6. *The cell structure method is applicable to general, non–autonomous, nonlinear systems of the form $\dot{x} = f(x,t)$, $x \in \mathbb{R}^n$ with the only requirement that f is periodic with respect to (a part of) the state vector x. For further details see [30, Chapter 8].*

VI. Main Result: Almost Global Attractivity

To streamline the presentation of our main result, it is convenient to introduce the following functions and quantities. Given the equilibrium values θ^s and ω^s, define the functions

$$\begin{aligned} q(\tilde{\theta}) &:= c\int_0^{\tilde{\theta}} \left[\sin(\theta^s - \phi + s) - \sin(\theta^s - \phi)\right] ds, \\ g(\lambda) &:= 4\left(R - \frac{L\lambda}{2}\right)\left[((L\omega^s)^2 + R^2)(D - \frac{J\lambda}{2}) - \frac{2\epsilon_{\min}}{\lambda}\right], \end{aligned}$$

with c and ϕ defined in (12) and (35), respectively, and where the constant ϵ_{min} is given by

$$\epsilon_{\min} := \inf\left\{\epsilon \in \mathbb{R}_{>0} \,|\, q(\tilde{\theta}) \leq \frac{\epsilon}{2}\tilde{\theta}^2,\ \forall \tilde{\theta} \in \mathbb{R}\right\}. \tag{39}$$

The lemma below shows that the infimum above is indeed achievable, and provides an explicit, though conservative, upper bound $\bar{\epsilon}$ for $\epsilon_{\min}$.

Lemma 1. *Consider the function*

$$h(\tilde{\theta}) = q(\tilde{\theta}) - \frac{\bar{\epsilon}}{2}\tilde{\theta}^2. \tag{40}$$

For all $\bar{\epsilon} > c$ we have that $h(\tilde{\theta}) \leq 0$ for all $\tilde{\theta} \in \mathbb{R}$.

Proof. Straight-forward calculations yield

$$q(\tilde{\theta}) = c[-\cos(\theta^s - \phi + \tilde{\theta}) - \sin(\theta^s - \phi)\tilde{\theta} + \cos(\theta^s - \phi)].$$

Hence, the function h in (40) is similar to a parabola which opens downward. The critical points of h are attained at values of $\tilde{\theta}^*$ satisfying

$$\frac{\partial h}{\partial \tilde{\theta}}\Big|_{\tilde{\theta}=\tilde{\theta}^*} = c[\sin(\theta^s - \phi + \tilde{\theta}^*) - \sin(\theta^s - \phi)] - \bar{\epsilon}\tilde{\theta}^* = 0. \quad (41)$$

It follows from the mean value theorem that

$$\sin(\theta^s - \phi + \tilde{\theta}^*) - \sin(\theta^s - \phi) \leq |\tilde{\theta}^*|.$$

Thus, for $\bar{\epsilon} > c$, the only solution of (41) is $\tilde{\theta}^* = 0$. Furthermore,

$$\frac{\partial^2 h}{\partial \tilde{\theta}^2}\Big|_{\tilde{\theta}=\tilde{\theta}^*} = c\cos(\theta^s - \phi + \tilde{\theta}^*) - \bar{\epsilon}.$$

which shows that for $\bar{\epsilon} > c \geq c\cos(\theta^s - \phi)$, $\tilde{\theta}^* = 0$ is a maximum of h, completing the proof.

□

The following assumption is fundamental to establish our claim.

Assumption 2. *There exists $\lambda_{max} > 0$—a point of local maximum of the function $g(\lambda)$—such that*

$$\begin{aligned} 2R &> \lambda_{max} L, \\ g(\lambda_{max}) &> (Lb\omega^s)^2. \end{aligned} \quad (42)$$

We are now ready to state our main result.

Theorem 1. *Consider the system* (11) *verifying Assumptions 1 and 2. The equilibrium point $(\theta^s, \omega^s, i_d^s, i_q^s)$ satisfying $|\theta^s - \phi| < \frac{\pi}{2}$ (modulo 2π) with ϕ defined in* (16) *is locally asymptotically stable and almost globally attractive,* i.e.*, for all initial conditions, except a set of measure zero, the solutions of the system* (11) *tend to that equilibrium point.*

Proof. Assumption 1 ensures, via Proposition 1, that equilibrium points exist. From the derivations above it is clear that the gist of the proof is to verify the conditions of Propositions 2 and 3.

We begin by establishing the local asymptotic stability claim. From (15) and the definition of $q(\tilde{\theta})$ above it follows that

$$q(0) = 0, \quad q'(0) = 0, \quad q''(0) = c\cos(\theta^s - \phi)$$

and

$$\sin(\theta^s - \phi) = \mathcal{P}, \quad (43)$$

with $\mathcal{P}$ defined in (12). From Assumption 1 we have $|\mathcal{P}| < 1$, therefore, the equation (43) has two roots θ^s (modulo 2π) in the interval $[\phi, \phi + 2\pi)$. If $|\theta^s - \phi| < \frac{\pi}{2}$, then $q''(0) > 0$. This implies that the function V defined in (30) has a local minimum at the origin. Furthermore, the parameters λ and $\epsilon_{\min}$ only enter with negative sign in $g(\lambda)$. Hence, Assumption 2 implies that (42) is also satisfied for $\lambda = \epsilon_{\min} = 0$ (with $(\epsilon_{\min}/\lambda)|_{(0,0)} := 0$) which is exactly condition (26). Thus, $\dot{V} \leq 0$ and the zero solution of the system (28) is Lyapunov asymptotically stable (see Proposition 2). If $|\theta^s - \phi| > \frac{\pi}{2}$, then $q''(0) < 0$, and the zero solution of the system (28) is Lyapunov unstable.

To establish almost global attractivity of the asymptotically stable equilibrium point (modulo 2π), in the following we assume that the zero solution of the system (28) is Lyapunov unstable (and therefore $|\theta^s - \phi| > \frac{\pi}{2}$). Recall the sets Z_k defined in (38) and note that every intersection of sets Z_k is also invariant. The set Z_k is equal to Z_0 shifted in the coordinate $\tilde{\theta}$ by $2\pi k$ to the right since $\theta_k^s = \theta^s + 2\pi k$. Now,

$$\begin{aligned} Z_0 = &\{\chi \in \mathbb{R}^4 \ : \ \frac{L}{2}(u^2 + w^2) + \frac{J\tilde{\omega}^2}{2}((L\omega^s)^2 + R^2) \\ &+ q(\tilde{\theta}) - \frac{\epsilon}{2}\tilde{\theta}^2 \leq 0\}. \end{aligned} \quad (44)$$

From Lemma 1 we have that this set is nonempty. Next we check the condition of Proposition 3. To this end, we evaluate $\frac{d\bar{V}}{dt} + \lambda\bar{V}$ with $\bar{V}$ defined in (33). This yields

$$\begin{aligned} \frac{d\bar{V}}{dt} + \lambda\bar{V} = &- R[u^2 + w^2] - D((L\omega^s)^2 + R^2)\tilde{\omega}^2 \\ &+ \tilde{\omega}u\ Lb\omega^s\cos(\tilde{\theta} + \theta^s) - \tilde{\omega}w\ Lb\omega^s\sin(\tilde{\theta} + \theta^s) \\ &- \epsilon\tilde{\theta}\tilde{\omega} + \lambda[\frac{L}{2}(u^2 + w^2) + \frac{J\tilde{\omega}^2}{2}((L\omega^s)^2 + R^2) \\ &+ c\int_0^{\tilde{\theta}}[\sin(\theta^s - \phi + s) - \sin(\theta^s - \phi)]ds - \frac{\epsilon}{2}\tilde{\theta}^2] \\ \leq &(-R + \frac{L\lambda}{2})[u^2 + w^2] \\ &- ((L\omega^s)^2 + R^2)(D - \frac{J\lambda}{2})\tilde{\omega}^2 \\ &+ \tilde{\omega}u\ Lb\omega^s\cos(\tilde{\theta} + \theta^s) - \tilde{\omega}w\ Lb\omega^s\sin(\tilde{\theta} + \theta^s) \\ &- \epsilon\tilde{\theta}\tilde{\omega} - \frac{\lambda(\epsilon - \epsilon_{\min})}{2}\tilde{\theta}^2 \\ = &\begin{bmatrix} u & w & \tilde{\omega} & \tilde{\theta} \end{bmatrix} M_1 \begin{bmatrix} u & w & \tilde{\omega} & \tilde{\theta} \end{bmatrix}^\top, \end{aligned} \quad (45)$$

where the matrix M_1 is defined in (48). The matrix M_1 is negative definite if and only if $\epsilon > \epsilon_{\min}$ and the matrix M_2 defined in (49) is negative definite. Similarly to the matrix M defined in (32) the matrix M_2 is negative definite if and only if $2R > L\lambda$ and

$$4(R - \frac{L\lambda}{2})[(L\omega^s)^2 + R^2)(D - \frac{J\lambda}{2}) - \frac{\epsilon^2}{2\lambda(\epsilon - \epsilon_{\min})}] > (Lb\omega^s)^2. \quad (46)$$

We now proceed to prove the existence of the positive parameters ϵ and λ appearing in (46). The maximum of the left-hand side with respect to ϵ is attained at $\epsilon = 2\epsilon_{\min}$. For this choice, the inequality (46) takes the form

$$4(R - \frac{L\lambda}{2})[((L\omega^s)^2 + R^2)(D - \frac{J\lambda}{2}) - \frac{2\epsilon_{\min}}{\lambda}] > (Lb\omega^s)^2. \quad (47)$$

Consider the following polynomial

$$f(\lambda) := ((L\omega^s)^2 + R^2)(D\lambda - \frac{J\lambda^2}{2}) - 2\epsilon_{\min},$$

and denote by λ_1 its smallest root, that is,

$$\lambda_1 = \frac{D - \sqrt{D^2 - \frac{4J\epsilon_{\min}}{(L\omega^s)^2 + R^2}}}{J}.$$

$$M_1 = \begin{bmatrix} -R+\frac{L\lambda}{2} & 0 & \frac{Lb\omega^s\cos(\tilde{\theta}+\theta^s)}{2} & 0 \\ 0 & -R+\frac{L\lambda}{2} & \frac{-Lb\omega^s\sin(\tilde{\theta}+\theta^s)}{2} & 0 \\ \frac{Lb\omega^s\cos(\tilde{\theta}+\theta^s)}{2} & \frac{-Lb\omega^s\sin(\tilde{\theta}+\theta^s)}{2} & -((L\omega^s)^2+R^2)(D-\frac{J\lambda}{2}) & -\frac{\epsilon}{2} \\ 0 & 0 & -\frac{\epsilon}{2} & -\frac{\lambda(\epsilon-\epsilon_{\min})}{2} \end{bmatrix} \tag{48}$$

$$M_2 = \begin{bmatrix} -R+\frac{L\lambda}{2} & 0 & \frac{Lb\omega^s\cos(\tilde{\theta}+\theta^s)}{2} \\ 0 & -R+\frac{L\lambda}{2} & \frac{-Lb\omega^s\sin(\tilde{\theta}+\theta^s)}{2} \\ \frac{Lb\omega^s\cos(\tilde{\theta}+\theta^s)}{2} & \frac{-Lb\omega^s\sin(\tilde{\theta}+\theta^s)}{2} & -((L\omega^s)^2+R^2)(D-\frac{J\lambda}{2})+\frac{\epsilon^2}{2\lambda(\epsilon-\epsilon_{\min})} \end{bmatrix} \tag{49}$$

If $\lambda_1 < \frac{2R}{L}$, then on the interval $[\lambda_1, \frac{2R}{L}]$ there is a unique point $\lambda_{\max}$ of local maximum of the left-hand side in (47).

The derivations above, together with the definition of $g(\lambda)$, prove that the inequalities (42) of Assumption 2 ensure M_1 is negative definite. Hence, condition (34) is satisfied and therefore Proposition 3 implies that all solutions $(\theta, \omega, i_d, i_q)$ of the system (11) are bounded.

Furthermore, the terms in λ and $\epsilon_{\min}$ only appear with negative sign on the right-hand side of (47). In addition, we see from the matrices M_1 in (48) and M_2 in (49) that for $\lambda = \epsilon_{\min} = \epsilon = 0$, (47) reduces to (26). Hence, condition (47) only holds if condition (26) of Proposition 2 holds. Consequently, under Assumption 2, all solutions $(\theta, \omega, i_d, i_q)$ of the system (11) are bounded and tend to an equilibrium point.

Denote by A the Jacobian of the system (11) evaluated at an equilibrium point, *i.e.*,

$$A = \begin{bmatrix} 0 & 1 & 0 & 0 \\ \frac{b}{J}\zeta & -\frac{D}{J} & -\frac{b}{J}\sin(\theta^s) & -\frac{D}{J}\cos(\theta^s) \\ \frac{b}{L}\omega^s\cos(\theta^s) & \frac{b}{L}\sin(\theta^s) & -\frac{R}{L} & -\omega^s \\ -\frac{b}{L}\omega^s\sin(\theta^s) & \frac{b}{L}\cos(\theta^s) & \omega^s & -\frac{R}{L} \end{bmatrix},$$

where

$$\zeta = i_q^s\sin(\theta^s) - i_d^s\cos(\theta^s).$$

Note that with (15) and (16), we have that

$$\zeta = \frac{1}{\left(\frac{R}{L}\right)^2+(\omega^s)^2}\left(\frac{b(\omega^s)^2}{L} - \frac{1}{L}\cos(\theta^s-\phi)\sqrt{\left(\frac{R}{L}\right)^2+(\omega^s)^2}\right).$$

Direct computations yield

$$\det(A) = \frac{b\cos(\theta^s-\phi)}{J\sqrt{R^2+(L\omega^s)^2}}.$$

Recall that at the unstable equilibrium point $|\theta^s-\phi| > \frac{\pi}{2}$. Consequently, there $\det(A) < 0$. Since moreover A is a real-valued matrix of dimension 4, $\det(A) < 0$ implies that A has at least one positive real eigenvalue. Hence, by invoking [34, Proposition 11] we conclude that the region of attraction of the unstable equilibrium has zero Lebesgue measure. Thus, for all initial conditions, except a set of measure zero, the solutions of the system (11) tend to the stable equilibrium point. This shows that the latter is almost globally attractive and completes the proof. □

Remark 7. *Note that if $\mathcal{P} = 0$ (and therefore $|\theta^s-\phi| = \frac{\pi}{2}$) then $\epsilon_{\min} = 0$, and the inequality (47) is equivalent to (26).*

Remark 8. *The related analysis in [13] critically relies on imposing a specific value for the mechanical torque T_m and on the knowledge of the stationary rotor currents i_{dq}^s. Compared to this, we don't need to impose any specific value for T_m. Furthermore, our convergence conditions only depend on the steady-state value of ω^s and, through* (39)*, on the relative rotor angle θ^s, but are independent of the stationary rotor currents i_{dq}^s.*

VII. Numerical examples

A key question is whether the conditions imposed by the inequalities (42) of Assumption 2 are verified in a practical SMIB scenario. We investigate this issue via two numerical benchmark examples reported in the literature.

The first example is taken directly from [22] and represents a 5kW synchronverter. Note that in the example of [22] the rotor current $i_f < 0$. Thus, $b < 0$ and $c < 0$, see (12). In our notation, this corresponds to the (potentially) stable equilibrium being shifted by π. Indeed, conditions (12), (13) and (26) are satisfied for this example. Hence, the system (11) has two equilibria and the proof of Theorem 1 implies that the equilibrium with $|\theta^s-\phi| > \pi/2$ is *locally* asymptotically stable. In addition, inequalities (42) of Assumption 2 are satisfied with $\epsilon_{\min} = 82.12$ and $\lambda = 23.81$. Consequently, by Theorem 1, the equilibrium with $|\theta^s-\phi| > \pi/2$ is also an *almost globally* attractive equilibrium. This result coincides with the conclusions in [22].

The parameters for the second example are taken from [2, Examples 4.2 and 5.1] and are expressed in per unit (pu) including normalized time (for $\omega_{\text{Base}} = 2\pi 60$rad/sec), see Table I. The normalized total moment of inertia is given by $J = 3\cdot 2H\omega_{\text{Base}}$, where H is the inertia constant [2]. We assume a nominal damping coefficient of $D_{\text{nom}} = 3\cdot 2$ pu (see [2, Table D.1-D.5])[4]. Furthermore, we assume a field current $i_f = 1.15$ pu yielding an RMS amplitude of 1.029 pu for

[4]The scaling factor 3 in J and D originates from the following fact. In [2], the mechanical equation (5) is expressed in pu with respect to the 3-phase base power $S_{3\phi}$. Hence, the pu values of J, D, T_m and T_e are also expressed with respect to $S_{3\phi}$. In the model (5), the electrical torque T_e in (10) is expressed with respect to the single-phase power $\frac{S_{3\phi}}{3}$. Consequently, one way to match our model (5) with the parameters in [2] is to scale J and D by a factor 3, *i.e.*, to represent the mechanical equation (5) with respect to the power base $\frac{S_{3\phi}}{3}$.

the EMF e_{abc}, a line resistance of $R_e = 0.02$ pu and line inductance of $L_e = 0.4$ pu.

We start by evaluating *local* stability of equilibria of the system (11). To this end, we note that condition (26) of Proposition 2 is independent of T_m. Furthermore, condition (26) is satisfied for the chosen set of parameters if the damping coefficient is chosen as $D \geq 6.5 D_{\text{nom}}$. Hence, if $D \geq 6.5 D_{\text{nom}}$, then for *any* choice of T_m such that the inequality (13) is strictly satisfied, the system (11) has two equilibria and by Proposition 1 the equilibrium with $|\theta^s - \phi| < \pi/2$ is locally asymptotically stable.

Global attractivity can be ensured for the data given in Table I via inequalities (42) for damping factors $D \geq 10 D_{\text{nom}}$. In general, the specific damping factor highly depends on the SG model and, in particular, on how the amortisseur windings are considered in the SG model [2, Appendix D]. The SG model (11) used in the present paper does not consider explicitly amortisseur damping at all. In that case, it is reasonable to assume a higher damping factor of up to $3 \cdot 25$ pu [2, Appendix D], which clearly implies $D \geq 10 D_{\text{nom}}$.

To further illustrate our findings, we have evaluated the required damping factor D for inequalities (42) to be satisfied for a wide range of operating conditions for both examples discussed above. The results are shown in Fig. 2a for the example from [22] and in Fig. 2b for the example from [2, Examples 4.2 and 5.1]. In the numerical experiments, we have varied the rotor current i_f and the mechanical torque T_m, while keeping all other parameters constant. Note that varying T_m implies varying the steady-state machine loading. Therefore, we have chosen to plot in Fig. 2 the ratio of required damping D over the nominal damping D_{nom} versus the steady-state RMS amplitude $E^s = \sqrt{1/3} b \omega^s$ of the EMF e_{abc} defined in (1) and the steady-state electrical torque T_e^s defined in (10). All values are in pu and T_e is normalized with respect to the single-phase power base given in [22], respectively [2, Examples 4.2 and 5.1], *i.e.*, the rated torque corresponds to $T_e^s = 3.0$ pu. Recall that large SGs can usually only be loaded at their rated power if the amplitude of the EMF e_{abc} is higher than the rated voltage [35, Chapter 5]. This explains the employed range of values for E^s and the limited electrical torque T_e^s for low values of E^s in Fig. 2b.

The results show that for both examples the higher the EMF E^s, *i.e.,* the higher the rotor current i_f, and the higher the machine loading, *i.e.,* the higher T_e^s, the larger D needs to be in order to ensure that inequalities (42) are satisfied. The latter correlation is more distinct in Fig. 2b, than in Fig. 2a. This may be explained by the higher R/X-ratio of the example in Fig. 2a ($R/X = 0.11$) compared to that of Fig. 2b ($R/X = 0.01$), see Remark 5. The made observations coincide with the well-known power-angle characteristic of reduced-order SG models, which states that an SG is more likely to become unstable after a change in load the closer it is operated at its generation limit [32], [1].

TABLE I: Parameters of the system (11) taken from [2, Example 4.4]

Parameter	Numerical value in pu	Parameter	Numerical value in pu
ω^s	1	J	$3 \cdot 1786.94$
D_{nom}	$3 \cdot 2$	M_f	1.2656
R	0.0211	L	2.1
i_f	1.15	V	1

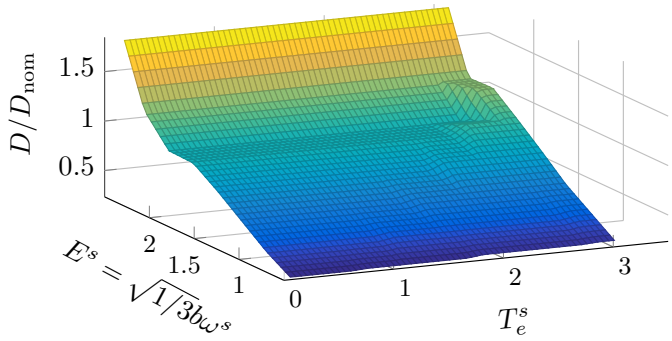

(a) Minimum required damping for inequalities (42) to be satisfied for different operating points for the example from [22]

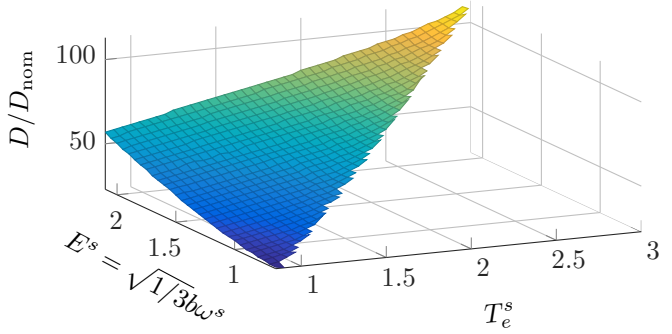

(b) Minimum required damping for inequalities (42) to be satisfied for different operating points for the example from [2]

Fig. 2: Evaluation of the required damping factor D relative to the nominal damping factor D_{nom} for inequalities (42) to be satisfied for a wide range of operating conditions for both investigated examples.

VIII. Conclusions

A complete analysis of existence and global attractivity of equilibria of a realistic SMIB model has been presented. More precisely, it is shown that (13)—with $\mathcal{P}$ defined in (12)—is a necessary and sufficient condition for existence of equilibria. Then, it is proven that if the inequalities (42) of Assumption 2 hold then almost all trajectories converge to a stable equilibrium point. Finally, the conservativeness of the estimates has been assessed via extensive numerical evaluations based on two benchmark problems.

We believe the presented results constitute a promising step towards the development of transient stability analysis methods for power system models with time-dependent transmission lines and physically more realistic SG models. Naturally, the main topic of our future research is the extension of the presented results to the multi-machine case. Given the "scalable" nature of the analysis tools employed here this

seems a feasible—albeit difficult—task.

ACKNOWLEDGEMENTS

The authors would like to thank the anonymous reviewers for many helpful comments that improved the quality and presentation of the manuscript.

REFERENCES

[1] J. Machowski, J. Bialek, and J. Bumby, *Power System Dynamics: Stability and Control*. J.Wiley & Sons, 2008.
[2] P. Anderson and A. Fouad, *Power System Control and Stability*. J.Wiley & Sons, 2002.
[3] J. D. Glover, M. S. Sarma, and T. J. Overbye, *Power System Analysis and Design*. Cengage Learning, 2011.
[4] P. Kundur, J. Paserba, V. Ajjarapu, G. Andersson, A. Bose, C. Canizares, N. Hatziargyriou, D. Hill, A. Stankovic, C. Taylor, T. Van Cutsem, and V. Vittal, "Definition and classification of power system stability IEEE/CIGRE joint task force on stability terms and definitions," *IEEE Transactions on Power Systems*, vol. 19, no. 3, pp. 1387–1401, Aug. 2004.
[5] G. Andersson, P. Donalek, R. Farmer, N. Hatziargyriou, I. Kamwa, P. Kundur, N. Martins, J. Paserba, P. Pourbeik, J. Sanchez-Gasca *et al.*, "Causes of the 2003 major grid blackouts in North America and Europe, and recommended means to improve system dynamic performance," *IEEE Transactions on Power Systems*, vol. 20, no. 4, pp. 1922–1928, Nov. 2005.
[6] S. V. Buldyrev, R. Parshani, G. Paul, H. E. Stanley, and S. Havlin, "Catastrophic cascade of failures in interdependent networks," *Nature*, vol. 464, no. 7291, pp. 1025–1028, April 2010.
[7] R. Rüdenberg, *Elektrische Schaltvorgänge und Verwandte Störungserscheinungen in Starkstromanlagen*. Julius Springer, Berlin, 1923.
[8] ——, *Transient Performance of Electric Power Systems*. McGraw-Hill, New York, 1950.
[9] V. Venkatasubramanian, H. Schattler, and J. Zaborszky, "Fast time-varying phasor analysis in the balanced three-phase large electric power system," *IEEE Transactions on Automatic Control*, vol. 40, no. 11, pp. 1975–1982, Nov. 1995.
[10] J. Schiffer, D. Zonetti, R. Ortega, A. Stankovic, T. Sezi, and J. Raisch, "A survey on modeling of microgrids–from fundamental physics to phasors and voltage sources," *Automatica*, vol. 74, pp. 135–150, Dec. 2016.
[11] P. Kundur, *Power System Stability and Control*. McGraw-Hill, 1994.
[12] S. Fiaz, D. Zonetti, R. Ortega, J. Scherpen, and A. van der Schaft, "A port-Hamiltonian approach to power network modeling and analysis," *European Journal of Control*, vol. 19, no. 6, pp. 477–485, Dec. 2013.
[13] S. Caliskan and P. Tabuada, "Compositional transient stability analysis of multimachine power networks," *IEEE Transactions on Control of Network Systems*, vol. 1, no. 1, pp. 4–14, March 2014.
[14] S. Y. Caliskan and P. Tabuada, "Uses and abuses of the swing equation model," in *54th IEEE Conference on Decision and Control*, Dec. 2015, pp. 6662–6667.
[15] H. Farhangi, "The path of the smart grid," *IEEE Power and Energy Magazine*, vol. 8, no. 1, pp. 18 –28, Jan. 2010.
[16] W. Winter, K. Elkington, G. Bareux, and J. Kostevc, "Pushing the limits: Europe's new grid: Innovative tools to combat transmission bottlenecks and reduced inertia," *IEEE Power and Energy Magazine*, vol. 13, no. 1, pp. 60–74, Jan. 2015.
[17] Q. Zhong and G. Weiss, "Synchronverters: Inverters that mimic synchronous generators," *IEEE Transactions on Industrial Electronics*, vol. 58, no. 4, pp. 1259 –1267, April 2011.
[18] K. Visscher and S. De Haan, "Virtual synchronous machines for frequency stabilisation in future grids with a significant share of decentralized generation," in *SmartGrids for Distribution, 2008. IET-CIRED. CIRED Seminar*, June 2008, pp. 1 –4.
[19] H.-P. Beck and R. Hesse, "Virtual synchronous machine," in *9th Int. Conf. on Electr. Power Quality and Utilisation.*, Oct. 2007, pp. 1 –6.
[20] T. Jouini, C. Arghir, and F. Dörfler, "Grid-friendly matching of synchronous machines by tapping into the DC storage," vol. 49, no. 22, Sep. 2016, pp. 192–197.
[21] V. Natarajan and G. Weiss, "Almost global asymptotic stability of a constant field current synchronous machine connected to an infinite bus," in *53rd IEEE Conference on Decision and Control*, Dec. 2014, pp. 3272–3279.
[22] ——, "A method for proving the global stability of a synchronous generator connected to an infinite bus," in *2014 IEEE 28th Convention of Electrical & Electronics Engineers in Israel*, Dec. 2014, pp. 1–5.
[23] ——, "Almost global asymptotic stability of a grid-connected synchronous generator," *arXiv preprint arXiv:1610.04858*, 2016.
[24] S. P. Bhat and D. S. Bernstein, "Finite-time stability of continuous autonomous systems," *SIAM Journal on Control and Optimization*, vol. 38, no. 3, pp. 751–766, July 2000.
[25] N. Barabanov, J. Schiffer, R. Ortega, and D. Efimov, "Almost global attractivity of a synchronous generator connected to an infinite bus," in *55th Conference on Decision and Control*, 2016, to appear.
[26] A. van der Schaft, *L_2-Gain and Passivity Techniques in Nonlinear Control*. Springer, 2000.
[27] G. Leonov, "On the boundedness of the trajectories of phase systems," *Siberian Mathematical Journal*, vol. 15, no. 3, pp. 491–495, May 1974.
[28] A. K. Gelig, G. Leonov, and V. Yakubovich, "Stability of nonlinear systems with nonunique equilibrium position," *Moscow Izdatel Nauka*, vol. 1, 1978.
[29] V. A. Yakubovich, G. A. Leonov, and A. K. Gelig, *Stability of Stationary Sets in Control Systems with Discontinuous Nonlinearities*. World Scientific Singapore, 2004.
[30] G. Leonov, "Phase synchronisation. Theory and applications," *Nonlinear Systems: Frequency and Matrix Inequalities*, vol. 67, no. 10.
[31] E. J. Noldus, "New direct Lyapunov-type method for studying synchronization problems," *Automatica*, vol. 13, no. 2, pp. 139–151, March 1977.
[32] J. J. Grainger and W. D. Stevenson, *Power System Analysis*. McGraw-Hill New York, 1994, vol. 621.
[33] J. W. Simpson-Porco, F. Dörfler, and F. Bullo, "Synchronization and power sharing for droop-controlled inverters in islanded microgrids," *Automatica*, vol. 49, no. 9, pp. 2603 – 2611, Sep. 2013.
[34] P. Monzón and R. Potrie, "Local and global aspects of almost global stability," in *45th IEEE Conf. on Decision and Control*, Dec. 2006, pp. 5120–5125.
[35] A. E. Fitzgerald, C. Kingsley, S. D. Umans, and B. James, *Electric Machinery*. McGraw-Hill New York, 2003, vol. 5.
[36] R. Teodorescu, M. Liserre, and P. Rodriguez, *Grid Converters for Photovoltaic and Wind Power Systems*. John Wiley & Sons, 2011, vol. 29.

APPENDIX

A. The dq-transformation

Following [2], [1], [36], [10], the dq-transformation employed in the model derivation of the SMIB model in Section II is stated. Let $x \in \mathbb{R}^3$ and $\varrho \in \mathbb{R}$. Consider the matrix $T_{dq} \in \mathbb{R}^{2\times 3}$,

$$T_{dq}(\varrho) := \sqrt{\frac{2}{3}} \begin{bmatrix} \cos(\varrho) & \cos(\varrho - \frac{2}{3}\pi) & \cos(\varrho + \frac{2}{3}\pi) \\ \sin(\varrho) & \sin(\varrho - \frac{2}{3}\pi) & \sin(\varrho + \frac{2}{3}\pi) \end{bmatrix}.$$

Then, $f_{dq} : \mathbb{R}^3 \to \mathbb{R}^2$,

$$f_{dq}(x, \varrho) = T_{dq}(\varrho)x$$

is called dq-transformation.

Nikita Barabanov received the M.Sc. and Ph.D. degrees in mathematics from Leningrad University, USSR, in 1976 and 1979, respectively, and the Dr.Sci. degree from Kiev Institute of Cybernetics, USSR, in 1990. Between 1979 and 2002 he has been with St.Petersburg Electrotechnical University, Russia, where he became a Full Professor in 1991. Since 2002 he is with the Department of Mathematics of North Dakota State University, Fargo, ND, USA. He had Visiting Professor positions with Ford Motor Company (USA), Newcastle University (Australia), Perth University (Australia), and Supelec (France). He is the author of more than 70 scientific papers in peer-reviewed journals. He was a supervisor of Ph.D. students in applied mathematics and control theory, and member of Ph.D. committees in Russia, Australia, France, and USA. He was a winner of many grants in control theory and differential equations. In 1980 he received the Award of the Leningrad Mathematical Society. He is a member of the Leningrad Mathematical Society and the American Mathematical Society.

Johannes Schiffer received his Diploma degree in Engineering Cybernetics from the University of Stuttgart, Germany, in 2009 and a Ph.D. degree (Dr.-Ing.) in Electrical Engineering from TU Berlin, Germany, in 2015. Currently he is a Lecturer (Assistant Professor) at the School of Electronic & Electrical Engineering, University of Leeds, UK. Prior to that, he has held appointments as research associate in the Control Systems Group (2011 - 2015) and at the Chair of Sustainable Electric Networks and Sources of Energy (2009 - 2011) both at TU Berlin. His current research interests include distributed control and analysis of complex networks with application to microgrids and power systems.

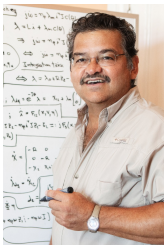

Romeo Ortega was born in Mexico. He obtained his BSc in Electrical and Mechanical Engineering from the National University of Mexico, Master of Engineering from Polytechnical Institute of Leningrad, USSR, and the Docteur D'Etat from the Politechnical Institute of Grenoble, France in 1974, 1978 and 1984 respectively.

He then joined the National University of Mexico, where he worked until 1989. He was a Visiting Professor at the University of Illinois in 1987-88 and at the McGill University in 1991-1992, and a Fellow of the Japan Society for Promotion of Science in 1990-1991. He has been a member of the French National Researcher Council (CNRS) since June 1992. Currently he is in the Laboratoire de Signaux et Systemes (SUPELEC) in Paris. His research interests are in the fields of nonlinear and adaptive control, with special emphasis on applications.

Dr. Ortega has published three books and more than 270 scientific papers in international journals, with an h-index of 71. He has supervised more than 30 PhD thesis. He is a Fellow Member of the IEEE since 1999 and has served as chairman in several IFAC and IEEE committees and editorial boards.

Denis Efimov (SM'11) received the Ph.D. degree in Automatic Control from the Saint-Petersburg State Electrical Engineering University (Russia) in 2001, and the Dr.Sc. degree in Automatic control in 2006 from Institute for Problems of Mechanical Engineering RAS (Saint-Petersburg, Russia). From 2000 to 2009 he was research fellow of the Institute for Problems of Mechanical Engineering RAS, Control of Complex Systems Laboratory. From 2006 to 2011 he was working in the LSS (Supelec, France), the Montefiore Institute (University of Liege, Belgium) and the Automatic control group at IMS lab (University of Bordeaux I, France). Since 2011 he joined the Non-A team at Inria Lille center. He is a member of several IFAC TCs and a Senior member of IEEE. His current research interests include nonlinear oscillation analysis, observation and control, switched and nonlinear system stability.